Relationship between steel shell temperature and nano $MgCr_2O_4$ addition on snorkel life time in Ruhrstahl-Heraeus vacuum steel refining units

N. Lotfian[1], A. A. Nourbakhsh*[2] , K. J. D. Mackenzie[3]

[1]Department of Materials Science and Engineering, Shahreza Branch, Islamic Azad University, Shahreza, Iran
[2]Arvin Dirgodaz Company, Isfahan Science and Technology Town, Isfahan, Iran
[3]MacDiarmid Institute for Advanced Materials and Nanotechnology, Victoria University of Wellington, New Zealand

Abstract

An investigation of the corrosion problems of the mag-chrome refractories used in the cylindrical component (snorkel) of Ruhrstahl-Heraeus (RH) vacuum degassing units is reported. The snorkel consists of a steel shell surrounded by a monolithic refractory and enclosing mag-chrome refractory bricks. Operational factors (degassing duration, time between heating cycles, number of heating cycles in a degassing sequence and the snorkel temperature) can overheat the steel shell and decrease the life of the snorkel. In the present study, the average temperature between the top and bottom of the steel shell was estimated by FDM (Finite Difference Method), indicating that thermal degradation due to creep will occur in the steel shell. In addition, the increasing number of hydrogen removal process during the degassing operation from the steel, the consumption of Fe-Si increased, producing more FeO and resulting in greater chemical corrosion of the refractory bricks. An investigation of these two mechanisms (thermal degradation and chemical corrosion) suggests that snorkel degradation could be mitigated by adjusting the number of daily heat sequences and cooling the steel shell, whereas the addition of $MgCr_2O_4$ nano additives to encourage spinel formation can be used to increase the hot modulus of rupture and increase the corrosion resistance.

Keywords: Snorkel, Mag-chrome, Refractories, Corrosion, Thermal shock.

1. Introduction

A Ruhrstahl-Heraeus (RH) degasser is a type of vacuum-refining furnace used in steel refining to remove hydrogen, nitrogen, carbon, and inclusions from the molten metal and improve the mixing of the molten steel in the ladle. This equipment is also used for the production of high-grade ultra low-carbon steels and silicon steels[1)]. Following the initial development of RH degassing technology in 1950-60, its application was established and new types of equipment continued to be developed[2)]. An integral component of an RH unit is the snorkel, a cylindrical part consisting of a shell of structural carbon steel such as grade SS400, surrounded by a monolithic alumina spinel refractory extending to the lower edge, and enclosing a lining of mag-chrome refractory bricks. The snorkel acts as the inlet for argon gas which pushes the molten steel into the vacuum chamber, removing dissolved impurity gases such as hydrogen from the steel. The strength of the carbon steel snorkel shell is extremely temperature-dependent, decreasing by about 10% when raised from room temperature to 800 °C, and losing its strength completely by 1077 °C. Since the RH vacuum refining process is carried out at high temperatures, and particularly since Al is added to the melt as an oxidizing agent to increase the melt temperature, deformation and degradation of the

*Corresponding author
Email:anourbakhs@yahoo.com
Address:Arvin Dirgodaz Company, Isfahan Science and Technology Town, Isfahan, Iran
1. Ph.D.
2. Assistant Professor
3. Professor

steel snorkel shell must be taken into account as a factor in the lifetime of the snorkel [3]. In addition to this thermal factor in the steel shell, the factors which affect to snorkel life time was categorized in 3 parts: a) thermal factors which considered the thermal shock due to changes of temperature, spalling of bricks and monolithic lining and Thermal difference between steel tube and refractory lining b)mechanical factor which included the Erosion due to hot steel circulation, erosion from gas movement, damage to outer snorkel from removal of adhering slag and finally c) chemical factor which devided to Acid and iron-rich slag attack, Slag infiltration and Corrosion by the oxidising and reducing atmosphere [4]. Czapka [5] showed that the snorkel lifetime depended on the operating conditions of the RH degasser (degassing duration, time between heating cycles, number of heating cycles in a refining sequence and the temperature of the steel shell, but did not comment on the relative importance of these various factors. However, high melt temperatures could cause the steel snorkel shell to overheat, resulting in cracking of the refractories with penetration of the molten steel, with wear of the refractories, especially near the edge of the snorkel exposed to the highest temperature [5]. The performance of the mag-chrome refractories has been the topic of much research aimed at improving their physical and mechanical properties and decreasing their corrosion rate. Thus, Azhari et al. [6] showed that the addition of Fe_2O_3 nanoparticles to mag-chrome refractories, increased direct bonding of the refractory matrix and improved its solid-state sintering. Golestanifard and Talimian [7] reported the effect of Cr_2O_3, Fe_2O_3, TiO_2 and boehmite additions to mag-chrome refractories and showed that nano-Cr_2O_3 and nano-Fe_2O_3 improved their corrosion resistance by strengthening the matrix. The oxide nano additives improved the resistance to liquid slag penetration by increasing the local viscosity of the slag at the penetration boundaries, possibly due to the dissolution of the nano-species in the attacking slag, thereby changing its viscosity [7]. Ghosh et al. [8] reported that the addition of ZrO_2 improved the physical and thermomechanical properties of mag-chrome composites were improved, while Zhao et al. [9] reported that the addition of nano-Fe_2O_3 to mag-chrome refractories improved the mechanical properties by facilitating direct bonding between the grains. Jingkun et al. [10]investigated the effect of TiO_2 and Al_2O_3 additives on the densification of mag-chrome refractories and showed their densification could be improved by the use of an optimum additive content. Lotfian et al. [11] reported the effect of nano-$MgCr_2O_4$ additions on mag-chrome refractories and showed that this nano additive improved both the physical and mechanical properties by facilitating the formation of secondary spinels which led to direct bonding.[11].

The aim of the present research was to improve the lifetime of the snorkels in RH vacuum degassing units by investigating two of the most important materials factors, namely the thermal degradation of the steel shell due to creep induced by increased temperatures at the top and bottom of the shell, and factors involved in the degradation/corrosion of the snorkel refractories. The thermal investigation consisted of statistical analysis and thermal simulation of the steel shell component of two used snorkels, while the incorporation of nano-sized $MgCr_2O_4$ was studied as a means of improving the corrosion resistance of the direct-bonded mag-chrome snorkel refractories.

2. Materials and method

2.1. Statistical investigation of two used snorkels

In this investigation, calculations were made on two used snorkels from the Mobarakeh Steel Company steelworks, Esfahan Province, Iran, which had experienced 82 and 97 heating cycles respectively under different operating conditions, to study the effect on the degradation/corrosion of the RH refractories, taking into account the respective operation parameters (number and duration of heating cycles, the percentage of hydrogen/carbon removal during the time in operation, the residual thickness of the mag-chrome refractories in the up leg/down leg of the snorkel, volume/pressure of the argon gas, depletion of Al from the melt and the steel shell temperature). All the statistical information for these two snorkels were obtained from the respective HMI (human and machine interface) data for all the melt cycles of these snorkels and the average and standard deviation of the results were reported.

2.2. Simulation and measurement of the steel shell temperature by the Finite Difference Method (FDM).

Since the steel shell temperature of the degasser snorkels determines their thermal expansion of the shell during operation, and is the reason for the formation of gaps between the internal mag-chrome refractory bricks and the spalling of the monolithic alumina spinel external refractory, the temperature of the steel shell under operating conditions is of great importance. The steady-state temperature of the steel shell was simulated by FDM.

The two-dimensional heat transfer equations in a cylindrical system are given by Eqs. 1 and 2 [12]:

$$\frac{\partial^2 T}{\partial r^2}+\frac{1}{r}\frac{\partial T}{\partial r}+\frac{\partial^2 T}{\partial Z^2}=0 \qquad \text{Eq. (1)}$$

$$\frac{(T_{i+1.j}-2T_{i.j}+T_{i-1.j})}{\Delta r^2}+\frac{1}{r}\left(\frac{T_{i+1.j}-T_{i-1.j}}{2\Delta r}\right)+ \qquad \text{Eq. (2)}$$

$$\frac{T_{i.j+1}-2T_{i.j}-2T_{i,j-1})}{(\Delta z)^2}=0$$

Where $T_{i,j}$ represents the temperature of point with

the coordinate (i,j), Δr represents the step size in the r direction (taken as 0.5), Δz represents the step size in the z direction (taken as 1) and represent the distance from the vertical axices (r=iΔr).

If Δz = 2Δr, equation 3 is used to determine the steady-state temperature as follows:

$$4iT_{i+1.j} - 10iT_{i.j} + 4iT_{i-1.j} + 2T_{i+1.j} - 2\,T_{i-1.j} + iT_{i.j+1} - 2iT_{i.j-1} = 0 \qquad \text{Eq. (3)}$$

Fig. 1 shows a schematic cutaway diagram of the refractory system in a snorkel, and Table 2 lists the physical data of the materials comprising the five radial regions marked in Fig. 1. Fig. 2 shows the node system of the snorkel, divided into equal increments in both the radial and axial directions for the purpose of the FDM analysis of the steel shell temperature.

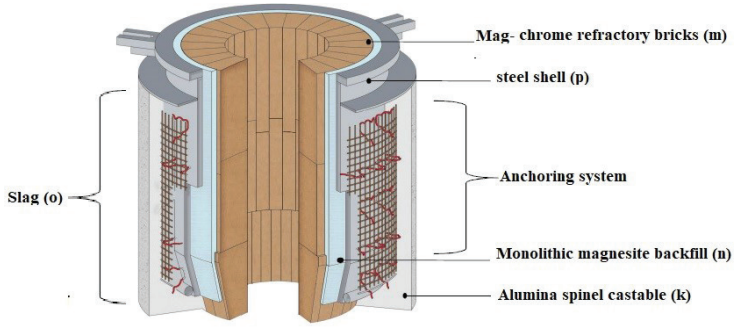

Fig. 1. Schematic cutaway diagram of the refractory system in a snorkel with the components in the radial direction labelled as in Table 1. Based on Kumar and Kremer [2].

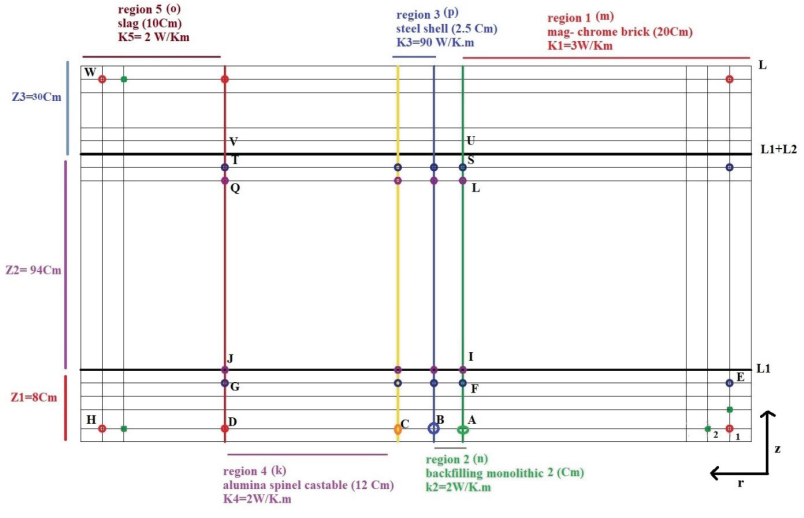

Fig. 2. Details of the node system in a snorkel on which the FDM calculations were based.

Table 1. Physical data for the regions of a snorkel in the radial direction, as marked in Figure 1.

Region number	Region symbol	Material	Thermal conductivity (W/m.K)	Thickness (Cm)
1	m	Mag-chrome refractory	3	20
2	n	Monolithic back filling (magnesite mortar)	2	2
3	p	Steel shell	30	2.5
4	k	Alumina spinel castable	2	12
5	o	Slag	2	10

The node system for the FDM calculations (Fig. 2) uses the coordinates of points within the snorkel in the radial (r) direction and the axial (z) direction, defined as follows:

In the radial direction, the zero point of the coordinate is at point 1 in region (m) (Table 1) and ends at point H in region (o). Thus, the coordinates of the points at the boundaries between the various snorkel components in the first level in the z direction are designated A, B, C and D, as shown in Table 2.

In this notation, point H, the final point in the radial direction before the slag boundary outside the snorkel, is defined as: H = m + n + p + k + o – 1.

The coordinate of each node is then defined by:
the node number in the r direction + (the z coordinate) × H

In this way, the position of each point is defined as in Table 3.

This results in H(L-1) points which are represented by individual equations that were solved by the Gauss-Seidel method [15] using the specially-written computer program given in the Supplementary Information section.

The FDM calculations of the temperatures within the snorkels were compared with actual temperature measurements of the different parts of the snorkel, carried out using an infrared thermal camera (Model 3I, Ritex 2012, United States).

2.3. Preparation of mag-chrome refractories containing $MgCr_2O_4$ nano additive spinel

The nanosized $MgCr_2O_4$ spinel additive for doping into the mag-chrome refractory bricks was prepared by the solution combustion synthesis method [16] using industrial-grade $Mg(NO_3)_2.6H_2O$ and $Cr(NO_3)_3.9H_2O$ (Nantong Zhongyixin Chemical Co). Citric acid was used as the chelating agent and fuel and the pH of the solution was adjusted to 6 using the ammonia solution. The self-combustion reaction was initiated by raising the temperature to 200 ℃.

The mag-chrome matrix was prepared from ~ 32% chromite from the Nehbandan mine (Iran) and ~68% of commercial Chinese dead burned magnesia (DBM97, Dashiqiao Yutong Co).

The $MgCr_2O_4$ nano-spinel was added to the magnesite-chrome refractories by dispersing 0.5 or 1 wt% of the nanopowder in an aqueous solution of calcium lignosulfonate, mixing for 30 min. then mixed with the

Table 2. Designations of the points in the radial direction at the boundaries within the various regions of the snorkel used for the FDM calculations.

Point name	Boundary in the snorkel structure
A	m (boundary between mag-chrome refractory and back filling monolithic)
B	m + n (boundary between backfilling monolithic and steel shell)
C	m + n + p (boundary between steel shell and alumina - spinel castable)
D	m + n + p + k (boundary between alumina-spinel castable and slag)
L1	boundary between Z1 and Z2
L1 + L2	boundary between Z2 and Z3
L	the boundary between snorkel and the ambient (liquid steel)

Table 3. Coordinates of selected points within the snorkel.

Point name	Coordinate	Point name	Coordinate
E	1 + (L1-1) H	G	m+n+p+k +(L1-1) H
F	m+ (L1-1)H	J	m+n+p+k +L1H
I	m+L1 H	Q	m+n+p+k + (L1+L2-2)
L	m + (L1+L2-2) H	T	m+n+p+k +(L1+L2-1) H
S	m+(L1+L2-1)H	V	m+n+p+k + (L1+L2)H
U	m+(L1+L2)H	W	m+n+p+k +o-1 + (L-1)H or W: H + (L-1)H

mag-chrome matrix for 30 min. to obtain a homogeneous distribution of the nanopowder. The samples were then uniaxially pressed at 120 MPa, dried overnight and fired at 1650 ℃ for 3 hr. in a shuttle kiln [11].

2.4. Corrosion testing of the magnesite-chrome refractories containing $MgCr_2O_4$ nano additive spinel

The corrosion resistance of samples MC0 and MC1 were carried out by the cup test according to the ASTM C621-84 standard method. The slag used in this test was taken from the entrance to an operating RH degasser and had the chemical composition shown in Table 5.

3. Results and discussion

3.1. Macroscopic investigation of a used snorkel

The schematic and experimental image of a used steel snorkel shell (Fig. 3) show how the melting of the steel shell (Fig. 3a) allows the liquid slag/metal phases to penetrate behind the refractories into the joints of the bricks (Fig. 3b). This highlights the most important cause of decreased snorkel lifetime.

Table 4. Description of mag-chrome refractory samples containing $MgCr_2O_4$ nano-additive.

Sample	Amount of $MgCr_2O_4$ nano-spinel additive
MC0	without $MgCr_2O_4$ nano-spinel additive
MC0.5	0.5% $MgCr_2O_4$
MC1	1% $MgCr_2O_4$

Table 5. Chemical composition of the RH degasser slag.

Oxide	SiO_2	$TiO_2+P_2O_5+V_2O_3$	MgO	Al_2O_3	CaO	MnO	FeO
Wt. %	3	<4	8	<3	51	7	24

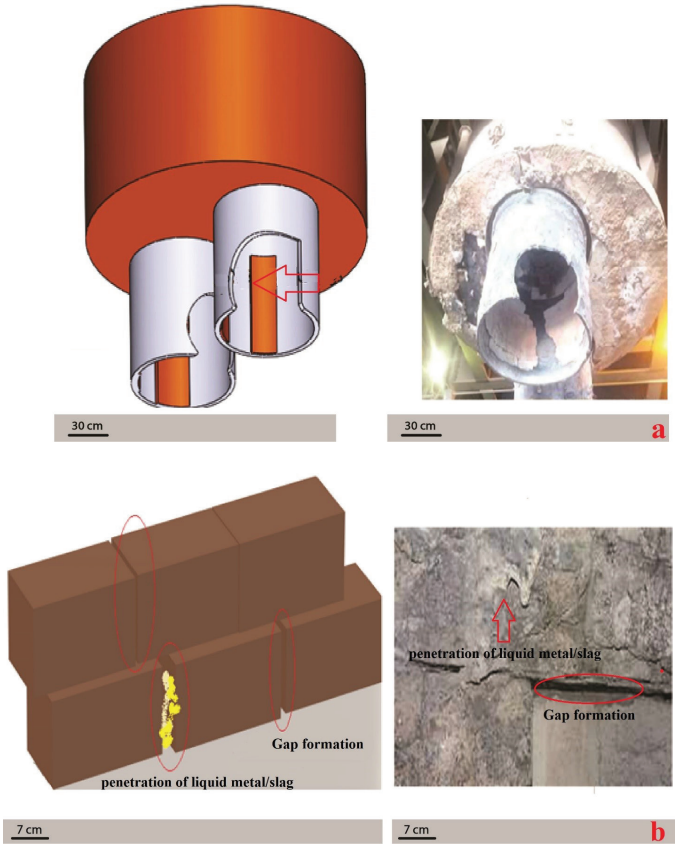

Fig. 3. Schematic and real image of a) melted portion of the steel shell after cooling (red arrow) b) penetration of the liquid phase behind the refractory at operating temperature, indicated by the red arrow.

3.2. FDM calculation of the steel shell temperature

The FDM method was used to provide a theoretical estimate of the steel shell temperature which was shown in Fig. 3 to be implicated in the mechanism by which penetration of the liquid slag/metal melt behind the refractories occurs. The FDM calculated two-dimensional temperature profile for a snorkel in the steady-state with a 20 cm thick refractory brick (Fig. 4) shows that the minimum temperature of the steel shell is about 828℃, while the maximum temperature is about 1518℃, giving an average temperature of about 1157℃ at different heights up the snorkel tube. Thus, in this temperature range, creep will occur due to the high temperature and expansion of the steel shell, allowing penetration of the liquid slag/metal phase between the refractory brick joints, leading to cracking and falling out of the bricks. The corresponding three-dimensional steady-state temperature profile of the snorkel is shown in Supplementary Fig. S1. The phenomena causing the degradation of the snorkel refractories are shown schematically in Fig. 5, which indicates that expansion and creep at the lower edge as a result of the higher temperature in this area causes the refractory joints to spread and crack, finally allowing the slag/steel melt to penetrate and degrade the mag-chrome refractories. These phenomena are consistent with suggestions by Nakamura et al. [3] and Czapka et al. [5].

To confirm this mechanism, the temperature of the various regions of the snorkel in operation was measured by an infrared thermometer (Fig. 6). This shows that the temperature of the snorkel in both the outlet and inlet region is >1000℃, at which temperature, creep of the steel shell is inevitable. This excellent agreement between the temperature simulation and actutal measurement confirms that the FDM method is a useful technique for estimating the temperature of the steel shell under various operating conditions.

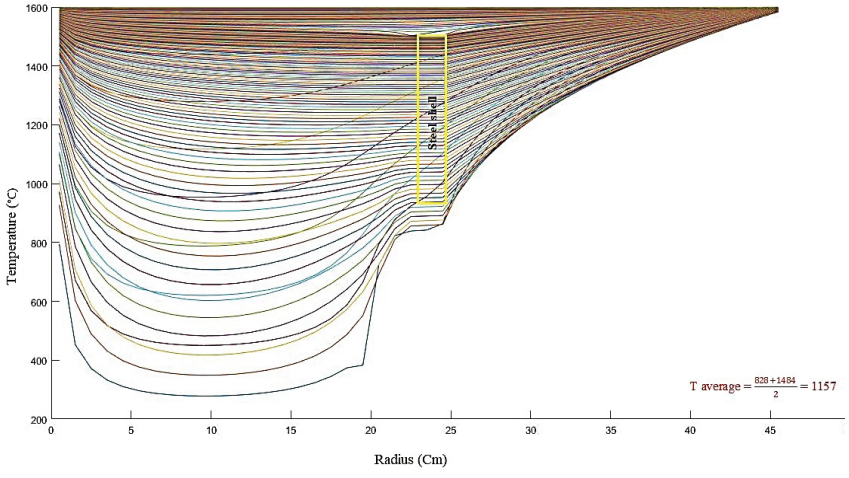

Fig. 4. Two-dimensional temperature profile of a snorkel in the steady-state calculated by FDM .

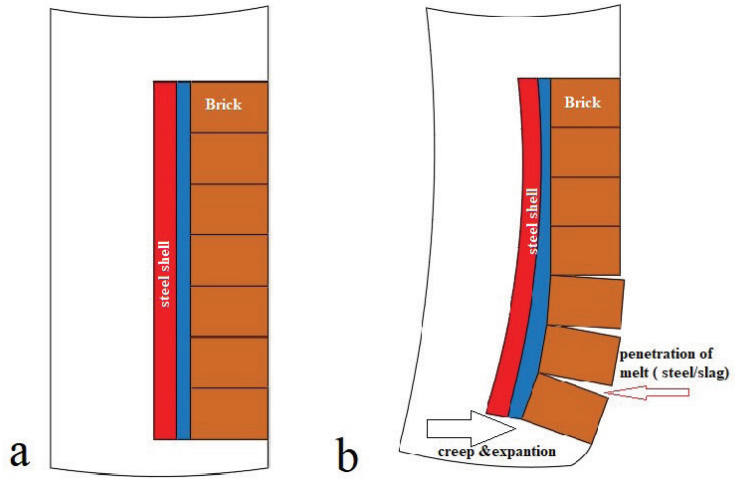

Fig. 5. Schematic diagram of a snorkel. a) before melting of the steel tube, b) after melting of the steel tube.

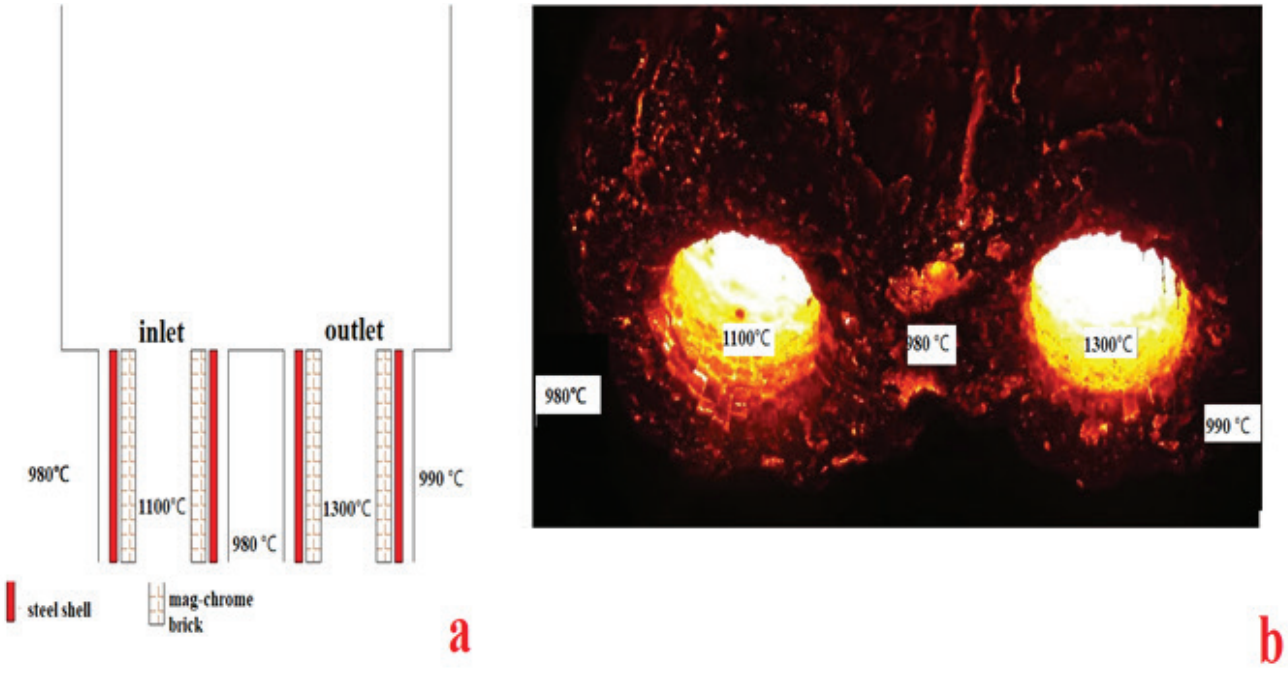

Fig . 6. Temperature measurement of the inlet and outlet steel snorkel shells under operating conditions. a) schematic representation, b) actual snorkels at temperature.

These results also show that the temperature of the steel shell increases continuously with the number of heating cycles per day. If the number of heating cycles per day is increased, the heat flux increases, increasing the temperature of the snorkel refractories ($\Delta\theta$) by the following equation:

$$Q = m\, c_p\, \Delta\theta \qquad \text{Eq. (4)}$$

Where Q = the heat energy (Joules), m = mass (kg), c p = specific heat at constant pressure (J/kg·K), $\Delta\theta$ = the temperature change (K).

Since the refractories are in contact with the steel shell, an increase the temperature of the refractories will increase the temperature of the steel shell.

Thus, one way of decreasing snorkel degradation would be to control the steel shell temperature by adjusting the number of heating cycles per day to allow the lower edge of the shell to cool between heating cycles.

3.3. Statistical data on the effect of the operating conditions on the corrosion of the two used snorkels.

The actual parameters associated with the performance of the used snorkels 1 and 2 studied in this investigation are shown in Table 6. The corresponding corrosion profiles of both snorkels are shown in Figures S2 of the Supplementary Information.

Table 6. Parameters associated with the performance of the used snorkels.

Parameter	Snorkel 1	Snorkel 2
Number of heating cycles (snorkel lifetime)	97	82
Residual thickness cm (inlet)	8	9.75
Residual thickness cm (outlet)	11	11.75
Heating time (min)	2377	2524
Stopped time (min)	6840	4170
Carbon removal (%)	23	28
Hydrogen removal (%)	77	72
Fe-Si (kg)	4500	6000
Al consumption per heating (kg)	87	84
Argon consumption per heating (m^3)	31	16
Oxygen consumption per heating (m^3)	38	26

These operational results show:

1. Since the refractory and melt are in equilibrium, the average degree of refractory corrosion in the inlet section is higher than in the outlet section, possibly due to the fact that the Ar used at the inlet for blowing decreases the equilibrium oxygen pressure of the melt, although the oxygen pressure of refractory remains unchanged, so that the oxygen activity of the refractory is higher than that of the melt, leading to corrosion of the refractory [17].
2. Although the average residual refractory thickness is the same in both snorkels, they had different lifetimes. This may reflect the two main problems in the RH degasser snorkel, namely, thermal degradation and chemical corrosion. We have therefore introduced two indices to define these effects, namely a thermal degradation (H-S) index and a chemical corrosion (FeO) index.

3.3.1. Thermal degradation (H-S) index

We define the H-S index as the ratio of the processing time to the stopped time in the operating cycle and represents the time during which the snorkels are in contact with the melt (Eq.5).

H-S index = processing time / stopped time Eq. (5)

Thus, the H-S index for snorkel 2 is 0.6 and the H-S index for snorkel 1 is 0.3, indicating that snorkel 2 will have been in contact with the melt for a longer time than snorkel 1, and will, therefore, have been subjected to a higher temperature, leading to a greater degree of creep and melting of the steel shell, and a shorter lifetime. To solve this problem, the H-S index could be decreased, for example, by increasing the stopped time and controlling the number of heating cycles per day.

3.3.2. Chemical corrosion (FeO) index

The chemical corrosion of the mag-chrome refractories with consequent penetration of molten material into the refractories is due to liquid phase formation resulting from the presence of Fe- Si in the melt (Fig. 3b). We express this effect in terms of the FeO index, which defines the amount of Fe-Si present. With increasing Fe-Si content (a higher FeO index), the lifetime of the refractories will be shortened because of the increased formation of the liquid phases. Thus, the greater amount of Fe- Si (higher FeO index) in snorkel 2 compared to snorkel 1 indicates that the lifetime of the snorkel 2 refractories will be shorter than that of snorkel 1. Although the Fe-Si content is an intrinsic property of the melt, its effect on the refractory bricks can be mitigated by the addition of $MgCr_2O_4$ nano spinel to enhance the texture of the magnesite-chrome refractories [11]. The effect of such an addition on the physical properties of the refractory is summarized in Table 7, indicating a significant improvement in the hot modulus of rupture (HMOR), an indicator of corrosion resistance, due to increase secondary spinel phase formation which affected on high temperature mechanical properties and corrosion resistance by the addition of 1% $MgCr_2O_4$ [11]. This is confirmed by SEM (Fig. 7) which shows the formation of a secondary spinel phase in sample MC1which approved by EDX analysis of selected area is shown in Fig 7d. In vew of the beneficial effect of a 1% $MgCr_2O_4$ addition, a corrosion resistance cup test was carried out on this sample, and, for comparison, on the sample without the nano-spinel addition.

3.4. Corrosion resistance cup tests of mag-chrome refractories containing $MgCr_2O_4$ nano-spinel

The results of the corrosion resistance cup tests of the mag-chrome refractory containing 1 wt% $MgCr_2O_4$ nano-spinel are shown in Table 8 and Fig. S3 and S4 in the supplementary information. These show a significant reduction in the diameter of the cup indentation in the sample containing the 1% $MgCr_2O_4$ addition, and correspond to an improvement of 8% in the corrosion resistance of the refractory. Thus, the addition of 1 wt% $MgCr_2O_4$ nano-spinel to the mag-chrome refractory suggests a practical and facile method for mitigating the effect of a high value of the FeO index on the performance of the snorkels.

Table 7. Physical and mechanical properties of mag-chrome refractories containing $MgCr_2O_4$ nano-spinel additions [11]

Sample	Permanent linear change (%)	Bulk density (g/cm^3)	Apparent porosity (%)	Cold crushing strength (MPa)	HMOR (MPa)
MC0	1.38	2/57	29/71	67.50	5.48
MC0.5	1.39	2/67	26/49	82.80	5.83
MC1	1.39	2/68	26/29	81.50	5.91

Table 8. Cup test results.

Sample	Cup diameter before the test (cm)	Diameter after the test (cm)
MC 0	2.00	2.26
MC 1	2.00	2.10

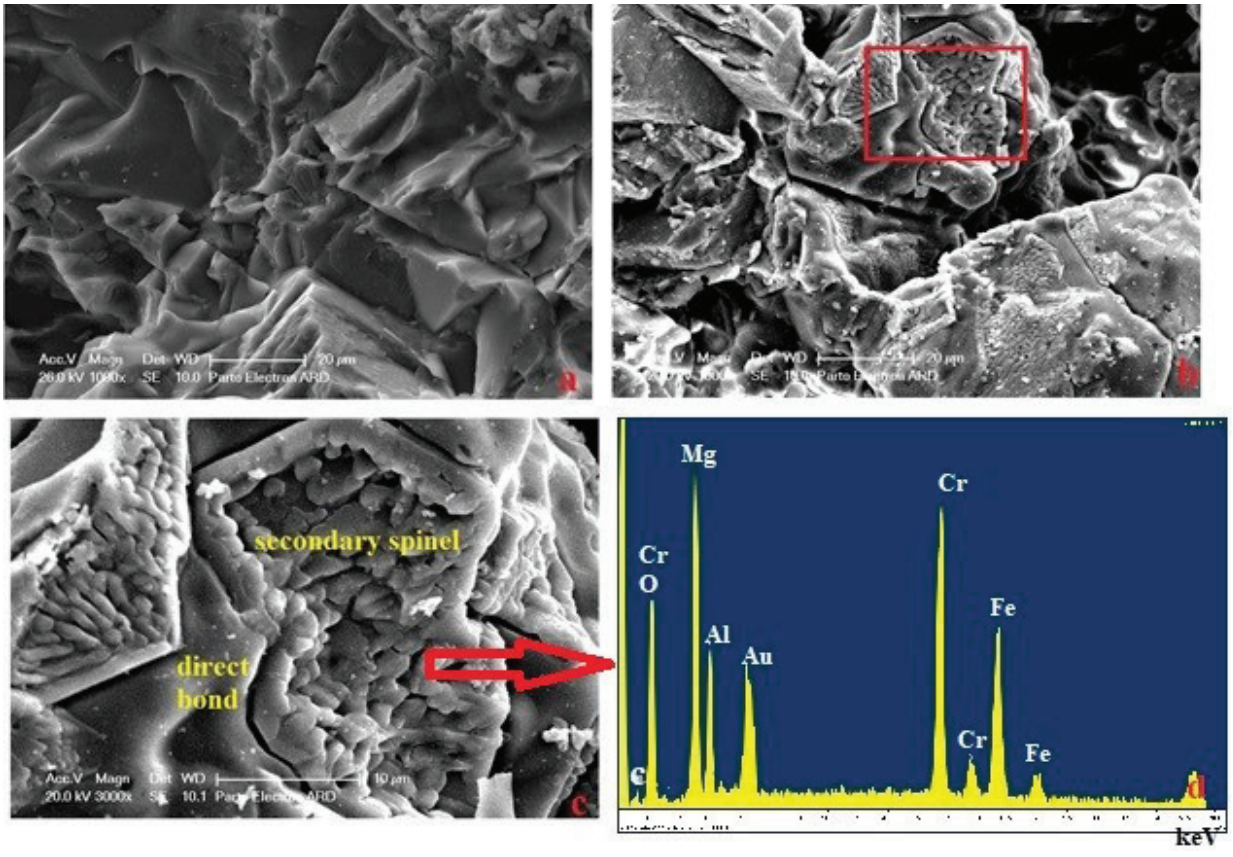

Fig . 7. SEM micrographs of mag-chrome refractories containing MgCr2O4 nano-spinel additions. a) sample MC0 (×1000), b) sample MC1 (×1000) c) region of sample MC1 (×3000) outlined in red in (b) d) EDX analysis of selected area.

4. Conclusions

- One of the two main factors affecting the lifetime of the snorkel components of RH vacuum degassing units is shown by microscopic investigation to be thermal degradation and melting of the steel shell, causing it to creep and allow penetration of melt phases behind the refractories. A second factor is the chemical corrosion of the mag-chrome refractories.
- As shown by measurement and thermal simulation by the FDM method, thermal degradation of the snorkel occurs when the steel shell temperature increases, causing expansion of the shell and penetration of the liquid phase into the refractory bricks, causing them to crack and fall out. This phenomenon was described by an H-S index, the ratio of the processing time to the stopped time, defining the time during which the snorkels are in contact with the melt. The effects of thermal degradation could be mitigated if the H-S index is lowered, for example, by adjusting the daily operating schedule to allow the steel shell to cool between heating sequences.
- Chemical degradation of the magnesite-chrome refractories is due to the high amount of FeO in the melt; this causes the formation of liquid phases which corrode the mag-chrome refractories. To solve this problem, reinforcement of the refractory brick by the addition of nano spinels additives is suggested.

Acknowledgments:

The authors thank members of the Materials Science Laboratory of the Islamic Azad University of Shahreza for their helpful contribution to this work.

References:

[1] L. Zhang, F. Li: Miner. Metal. Mater. Soc., 66 (2014), 1227.

[2] Kumar, S, Kremer: 14th Biennial Worldwide Congress Unitecr 2015, Vienna, Austria, 2015 .

[3] Y.Nakamura, S.Hosohara, K. Takahashi : 15th Biennial Worldwide Congress Unitcer 2017, Santiago, Chile, (2017), 293.

[4] K. Subramaniam, A. Kremer: Stahl and Eisen., 129 (2009) ,47.

[5] Z.Czapka, J. Szczerba, W.Zelik : Proc. Unitcer. 2013, Victoria, Canada, (2013),761.

[6] A.Azhari, F. Golestani-Fard, H. Sarpoolak: J. Eur.

Ceram. Soc., 29(2009), 2679.
[7] F. Golestani-Fard, A. Talimian, : Refractories World Forum., 6(2014), 93.
[8] A.Ghosh, M.K Haldar, S.K. Das : Ceram. Int., 33(2007), 821.
[9] Z. Huizhong, H. Shoutian, W. Houzhi: Unitcer 2003, Osaka, Japan ,(2003), 284.
[10] Y. Jingkun, D.Shuping, G. Xinkul:. Unitcer 2003, Osaka, Japan (2003),102.
[11] N.Lotfian, A.A. Nourbakhsh, S.N. Mirsattari, A. Saberi, K.J.D: Ceram. Int., 46(2020), 747.
[12] J.P. Holman: Heat Transfer, Tenth edition, McGraw-Hill ,New York, NY 10020, (2010).
[13] W. Yan, G. Wu, S. Ma, S. Schafföner, Y. Daia, Z. Chen, J. Qi, N. Li: J. Eur. Ceram. Soc., 38(2018;), 4276.
[14] Verlag Stahleisen.; Verein Deutscher Eisenhüttenleute.: Slag atlas, Dusseldorf : Verlag Stahleisen GmbH, cop. (1995).
[15] A. Etemad, G. Dini, S. Schwarz, Materials Science and Engineering: A, 742(2019), 27.
[16] S. Li, X. Jia, Y. Qi : J. Adv. Mater. Res., 284(2011), 730.
[17] K.Kwong, A.Petty, J. Bennett, R. Krabbe, H. Thomas : Appl. Ceram. Technol., 4(2007), 503

Supplementary information

Computer program for calculation of the temperature profile by the FDM method

```
k2=2;k4=2;k1=3;k3=10;z1=8;z2=94;z3=30;k5=2;k6=3;
Le=z1+z2+z3;
%Re=input('length in R direction')
hr=input('step size R direction');
hz=input('step size in z direction');
L=Le/hz;L1=z1/hz;L2=z2/hz;L3=z3/hz;
%R=input('segments number in R direction')
%m=input('segments number in R direction; part #1');n=input('segments number in R direction;part #2')
%p=input('segments number in R direction; part #3');k=input('segments number in R direction;part #4');
m=20/hr;n=2/hr;p=2.5/hr;k=12/hr;o=10/hr;
H=m+n+p+k+o-1;Dr=hr;Dz=hz;D=Dr/Dz;
A=zeros(H*(L-1));b(1:H*(L-1))=0;
% Basic Part
for j=(2+H):(H*(L-2)-1)
if rem (j,H)==0
 M=H;
else
M=rem(j,H);
End
 if  j~=1:H: H*(L-2)+1
 if   j~= H:H: H*(L-1)
 if   j~=m+n+p+k:H:m+n+p+k+(L-2)*H
if j~=m+(L1-1)*H:H:m+(L1+L2-1)*H
if j~=m+n+(L1-1)*H:H:m+n+(L1+L2-1)*H
if j~=m+n+p+(L1-1)*H:H:m+n+p+(L1+L2-1)*H
%if j~=1+(L1-1)*H:m+n+p+k+(L1-1)*H
%if j~=1+(L1+L2-1)*H:m+n+p+k+(L1+L2 -1)*H
A(j,j)= -2*(1+D^2);A(j,j-1)= 1-1/(2*M);A(j,j+1)= 1+1/(2*M);A(j,j+H)= D^2;
A(j,j-H)= D^2;
end
end
end
end
end
end
%end
end
%end
%Boundaries
for j=2:H-1
if rem (j,H)==0
M=H;
Else
 M=rem(j,H);
end
if j~=m+n+p+k
A(j,j)= -2*(1+D^2);A(j,j-1)= 1-1/(2*M);A(j,j+1)= 1+1/(2*M);A(j,j+H)= D^2;
b(j)=-1600*D^2;
end
end
for j=H*(L-2)+2:H*(L-1)-1
if rem (j,H)==0
M=H;
 else
M=rem(j,H);
end
if  j~=m+n+p+k+(L-2)*H
A(j,j)= -2*(1+D^2);A(j,j-1)= 1-1/(2*M);A(j,j+1)= 1+1/(2*M);A(j,j-H)= D^2;
b(j)= -1600*D^2;
end
end
for j=m+n+p+k+o:H:H*(L-3)+1
if rem (j,H)==0
 M=H;
else
M=rem(j,H);
end
%if j~=1+(L1-1)*H
```

```
A(j,j)= -2*(1+D^2);A(j,j+1)= 1+1/(2*M);A(j,j+H)= D^2;A(j,j-H)= D^2;
b(j)=-1600*(1-1/(2*M));
end
%end
for j=2*H:H:H*(L-2)
if rem (j,H)==0
 M=H;
else
M=rem(j,H);
end
A(j,j)= -2*(1+D^2);A(j,j-1)= 1-1/(2*M);A(j,j+H)= D^2;A(j,j-H)= D^2;
b(j)=-1600*(1+1/(2*M));
end
%interface
for j=m+L1*H:H:H*(L1+L2-2)+m
A(j,j)= k1+k2;A(j,j-1)= -k1;A(j,j+1)= -k2;b(j)=0;A(j,j+H)=0;A(j,j-H)=0;
end
for j=m+n+L1*H:H:H*(L1+L2-2)+m+n
A(j,j)= k3+k2;A(j,j-1)= -k2;A(j,j+1)= -k3;b(j)=0;A(j,j+H)=0;A(j,j-H)=0;
end
for j=m+n+p+L1*H:H:H*(L1+L2-2)+m+n+p
A(j,j)= k4+k3;A(j,j-1)= -k3;A(j,j+1)= -k4;b(j)=0;A(j,j+H)=0;A(j,j-H)=0;
end
for j=m+n+p+k:H:m+n+p+k+(L-2)*H
if j<m+n+p+k+(L1-1)*H+1
A(j,j)=k1+k5;A(j,j-1)=-k1;A(j,j+1)=-k5;b(j)=0;
end
if j>m+n+p+k+(L1-1)*H&j<m+n+p+k+(L1+L2-1)*H
A(j,j)=k4+k5;A(j,j-1)=-k4;A(j,j+1)=-k5;b(j)=0;
end
if j>m+n+p+k+(L1+L2-1)*H
A(j,j)=k6+k5;A(j,j-1)=-k6;A(j,j+1)=-k5;b(j)=0;
end
end
%visual points
for j=1+(L1-1)*H:m+(L1-1)*H
A(j,j)=k1+k2;A(j,j-H)=-k2;A(j,j+H)=-k1;b(j)=0;
end
%for j=m+(L1-1)*H+1:m+n+(L1-1)*H
%A(j,j)=k2+k2;A(j,j-H)=-k2;A(j,j+H)=-k2;b(j)=0;
%end
for j=m+n+(L1-1)*H:m+n+p+(L1-1)*H
A(j,j)=k2+k3;A(j,j-H)=-k2;A(j,j+H)=-k3;b(j)=0;
end
%for j=m+n+p+(L1-1)*H+1:m+n+p+k+(L1-1)*H
%A(j,j)=k2+k4;A(j,j-H)=-k2;A(j,j+H)=-k4;b(j)=0;
%end
%for j=1+(L1+L2-1)*H:m+(L1+L2-1)*H
%A(j,j)=k1+k6;A(j,j-H)=-k1;A(j,j+H)=-k6;b(j)=0;A(j,j+1)=0;A(j,j-1)=0;
%end
for j=m+(L1+L2-1)*H:m+n+(L1+L2-1)*H
A(j,j)=k2+k6;A(j,j-H)=-k2;A(j,j+H)=-k6;b(j)=0;A(j,j+1)=0;A(j,j-1)=0;
end
for j=m+n+(L1+L2-1)*H+1:m+n+p+(L1+L2-1)*H
A(j,j)=k6+k3;A(j,j-H)=-k3;A(j,j+H)=-k6;b(j)=0;A(j,j+1)=0;A(j,j-1)=0;
end
for j=m+n+p+(L1+L2-1)*H+1:m+n+p+k+(L1+L2-1)*H
A(j,j)=k6+k4;A(j,j-H)=-k4;A(j,j+H)=-k6;b(j)=0;A(j,j+1)=0;A(j,j-1)=0;
end
A(1,1)= -2*(1+D^2);A(1,2)= 1+1/(2*rem(1,H));A(1,H+1)= D^2;
b(1)=-1600*(D^2+(1-1/(2*rem(1,H))));
A(H,H)= -2*(1+D^2);A(H,H-1)= 1-1/(2*H);A(H,2*H)= D^2;
b(H)=-1600*(D^2+(1+1/(2*H)));
A(H*(L-2)+1, H*(L-2)+1)=-2*(1+D^2);
A(H*(L-2)+1,H*(L-2)+2)= 1+1/(2*rem(H*(L-2)+1,H));
A(H*(L-2)+1,H*(L-2)+1-H)= D^2;
b(H*(L-2)+1)=-1600*(D^2+(1-1/(2*rem(H*(L-2)+1,H))));
A(H*(L-1), H*(L-1))=-2*(1+D^2);A(H*(L-1),H*(L-1)-1)= 1-1/(2*H);
A(H*(L-1),H*(L-1)-H)= D^2;b(H*(L-1))=-1600*(D^2+(1+1/(2*H)));
s=size (A)
ss=size(b)
%d=det(A);
T=A\b';
A;
%print
for i=1:H*(L-1)
if A(i, :)==zeros(1, H*(L-1));  i
end
end
for i=1:(L-1)
Te(i,1:H)=T(1+H*(i-1):H*i);
hold on
plot(hr:2*hr:H*hr,Te(i,1:2:H))
end
```

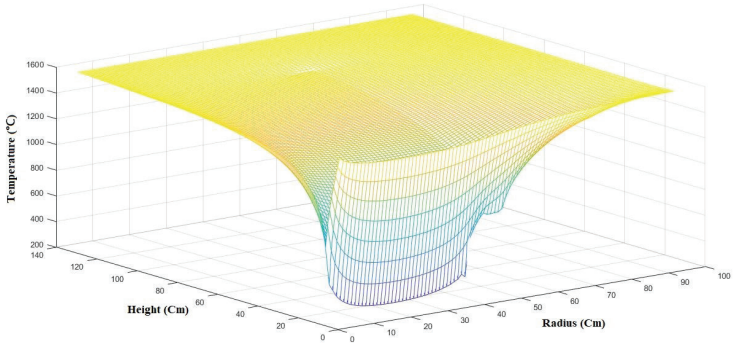

Fig.S1- three-dimensional temperature profile of a snorkel in the steady state.

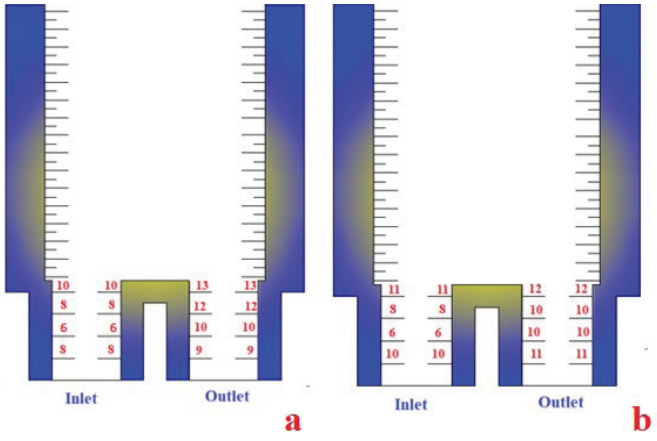

Fig. S2- The residual thickness profile of mag- chrome bricks in a) snorkel 1 b)snorkel 2.

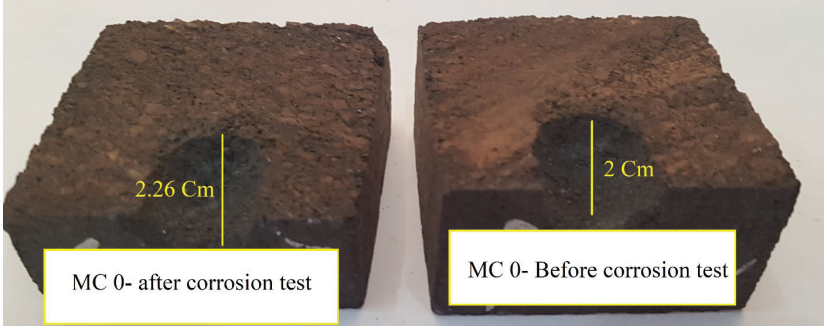

Fig. S3. Corrosion cup test analysis of sample MC 0.

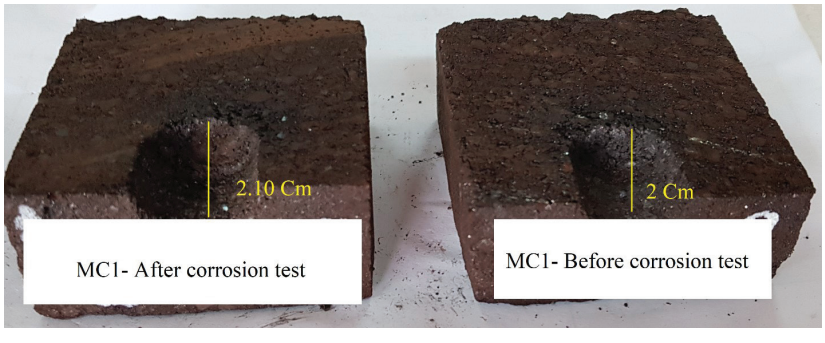

Fig. S4. Corrosion cup test analysis of sample MC 1.